

An Online Learning System for Wireless Charging Alignment using Surround-view Fisheye Cameras

Ashok Dahal, Varun Ravi Kumar, Senthil Yogamani, and Ciarán Eising, *Member, IEEE*

arXiv:2105.12763v1 [cs.CV] 26 May 2021

Abstract—Electric Vehicles are increasingly common, with inductive chargepads being considered a convenient and efficient means of charging electric vehicles. However, drivers are typically poor at aligning the vehicle to the necessary accuracy for efficient inductive charging, making the automated alignment of the two charging plates desirable. In parallel to the electrification of the vehicular fleet, automated parking systems that make use of surround-view camera systems are becoming increasingly popular. In this work, we propose a system based on the surround-view camera architecture to detect, localize and automatically align the vehicle with the inductive chargepad. The visual design of the chargepads is not standardized and not necessarily known beforehand. Therefore a system that relies on offline training will fail in some situations. Thus we propose an online learning method that leverages the driver’s actions when manually aligning the vehicle with the chargepad and combine it with weak supervision from semantic segmentation and depth to learn a classifier to auto-annotate the chargepad in the video for further training. In this way, when faced with a previously unseen chargepad, the driver needs only manually align the vehicle a single time. As the chargepad is flat on the ground, it is not easy to detect it from a distance. Thus, we propose using a Visual SLAM pipeline to learn landmarks relative to the chargepad to enable alignment from a greater range. We demonstrate the working system on an automated vehicle as illustrated in the video https://youtu.be/_cLCmkW4UYo. To encourage further research, we will share a chargepad dataset used in this work.

Index Terms—Automated Parking, Electric Vehicle Charging, Visual SLAM, Online Learning, Multi-Task Learning, Self Supervised Learning

I. INTRODUCTION

WITH predicted growth in the electric vehicle market over the next decade, with a market penetration of up to 42.5% by 2035 expected [1], wireless charging is seen as a key enabling technology and is now the subject of standardization [2]. Inductive charging is market-ready [3] but suffers due to driver behavior. Inductive charging efficiency is highly related to the charging coils’ position relative to one another, with a tolerance of approximately $\pm 10\text{cm}$ from the center points. In contrast, studies have shown that human parking accuracy is between 20 and 120cm longitudinally and 20 to 60cm laterally, with only 5% of vehicles parked within the tolerances for optimal efficiency [4]. It, therefore, becomes evident that automated chargepad alignment is vital for the

A. Dahal is with Valeo North America, Troy, MI, USA. E-mail: ashok.dahal@valeo.com.

V. Ravi Kumar is with Valeo Driving Assistance Research, Kronach, Germany. E-mail: varun.ravi-kumar@valeo.com.

S. Yogamani is with the Valeo Vision Systems, Tuam, Co. Galway, Ireland. E-mail: senthil.yogamani@valeo.com.

C. Eising is with the Department of Electronic and Computer Engineering, University of Limerick, Ireland. E-mail: ciaran.eising@ul.ie.

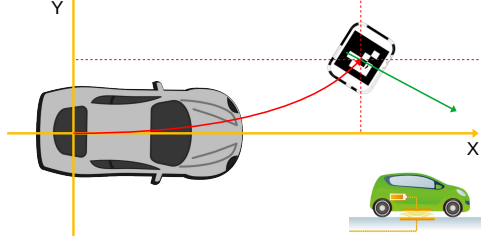


Fig. 1: Illustration of Chargepad Parking, including detection, localization, and alignment with automated driving. The positional alignment (indicated by the red line) and the angular alignment (green axis) are both important for optimal charging.

widespread uptake of wireless charging for electric vehicles. Chargepad alignment is exemplified in Figure 1.

Several solutions have been proposed to solve the problem of automated chargepad alignment. In [5], a system whereby additional hardware in the form of wireless sensors on the coils is proposed, with at least six sensors (three per coil) required. In [6], a set of *LC* sensors is proposed to be installed on the installed charging coil, enabling the detection of the direction that the electric vehicle must be driven for optimal alignment. Tiemann et al. [7] propose an ultra-wideband wireless alignment system based on IEEE 802.15.4a, and [8] propose a method of position detection based on the analysis of voltage differences in so-called search coils. In contrast, our proposal is based on using a set of surround-view cameras that are standard on many vehicles.

In parallel to the accelerated development of electric vehicles and wireless charging stations, wide field-of-view or fisheye cameras are becoming commonplace on vehicles, particularly for automated parking systems [9], a problem that is highly related to the problem of wireless charging station alignment. Of key importance is that the fisheye cameras provide video of the scene right up to the vehicle body, providing important near field sensing. Computer vision has been considered for chargepad alignment. For example, [10] propose a stereo vision-based approach. However, stereo vision systems suffer from field-of-view issues. They are typically unable to cover the vehicle’s near-field area. When the chargepad moves out of the camera’s view, one must rely on the vehicle odometry solely, which can lead to drift in the positional alignment.

In particular, fisheye cameras are commonly deployed on vehicles in a surround-view configuration [9], as stylized in Figure 2, with one camera at both the front and rear of the vehicle and on each of the wing-mirrors. Such camera networks have traditionally been deployed for viewing applications (e.g.,

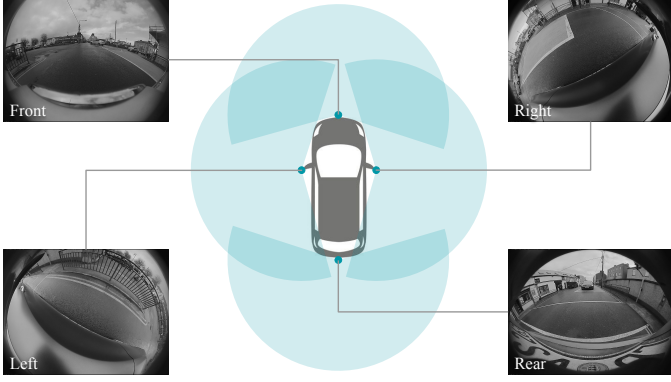


Fig. 2: **Illustration of a typical automotive surround-view system** consisting of four fisheye cameras located at the front, rear and on each wing-mirror.

[11] and many commercial surround-view products). However, surround-view cameras are increasingly focused on near field sensing, which can be used for low-speed applications such as parking or traffic jam assistance functions [12]. There is relatively less work on using convolutional neural networks for fisheye cameras. Recently, it has been explored for various tasks such as object detection [13], soiling detection [14], depth prediction [15], [16], [17], [18], SLAM [19] and in general for multi-task outputs [20]. As we shall see later, of particular interest for chargepad detection is the joint learning of object, depth, and semantic segmentation, which we shall deploy for the refinement of auto-annotation for online learning.

A problem with any visual approach to detecting the chargepad is that there are significantly different designs. An example of just a few is shown in Figure 3. As electric vehicles gain momentum, different OEMs come up with their version of electric vehicles and chargepad designs. As this is still in an early phase, the standardization of the chargepads has not been done yet. It may not happen due to aesthetic driving factors. In this paper, therefore, we propose an online self-supervised training method for solving the problem of the detection of unseen chargepads. An initial network is trained using a set of pre-defined chargepad types. If this fails for any chargepad alignment instance, the driver will need to align the vehicle with the chargepad manually. However, we propose a method to auto-annotate the chargepad by reversing the vehicle odometry to extract the location of the chargepad in recorded frames of video. We propose to solve accuracy issues with this approach by applying a refinement step to use semantic road segmentation and depth estimation to improve the localization of the chargepad in the video frames.

The remainder of this paper is structured as follows. In Section II, we discuss the proposed method, describing the multi-task learning (MTL) perception stack, the visual SLAM that we ultimately use for extending the range of the alignment algorithm, the online self-supervised learning method, and the overall system architecture proposal. We also describe a fiducial marker-based chargepad design. We then present a set of results that support our argument that this is an effective system for chargepad sensing and alignment in Section III.

II. PROPOSED METHODS AND ARCHITECTURE

In this section, we describe the different methods that contribute to the overall architecture. We describe an ArUco pattern-based chargepad design, which we use in the test dataset and which provides a baseline algorithm for our proposed approach. Then we describe the three task perception stack that outputs object detection, segmentation, and distance that are used in the online auto-annotation later. We discuss how we approach online learning for the chargepad. We discuss Visual SLAM approaches that can be used to extend the range of the alignment algorithm beyond the limited range of direct detection of the chargepad. Finally, we introduce our overall architecture, whereby we combine all of these elements.

A. Fiducial Marker Chargepad Design

Fiducial marker-based camera pose estimation or object detection and tracking are widely used in computer vision applications [21]. The configurable ArUco markers [22] can be used as a fixed object for detection and tracking purposes in challenging scenes where various objects are present simultaneously. They have good contrast with both bright and dark regions. Additionally, they do not have rotational symmetry, and as such, orientation information can be extracted. As camera sensors are widely used, their cost is coming down. At the same time, quality such as image resolution is going up. The increase of computation time with the increase of image resolution can be well handled using simple ArUco based patterns in object detection and tracking [23].

In this work, the architecture we design is not limited to ArUco patterns. In fact, having such patterns on the chargepad is non-desirable in OEM production, as they would not be considered aesthetically pleasing. However, using ArUco patterns is useful, as it gives a ground truth algorithm on which to base our development on. Therefore, our test data consists of chargepads with an ArUco pattern. The design of the chargepad pattern is demonstrated in Figure 4.

B. Near-field Perception Stack through Multi-Task Learning (MTL)

We derive the baseline MTL model from our recent work OmniDet [24], a six-task complete perception model for surround-view fisheye cameras. We focus on the three relevant perception tasks: object detection, semantic segmentation, and depth estimation. While we provide a short overview of the baseline model here, the reader is referred to [24] for more complete details. A high-level architecture of the model is shown in Figure 5. It comprises a shared ResNet18 [25] encoder and three decoders for each task. 2D bounding box detection task has the six important objects, namely *pedestrians*, *vehicles*, *riders*, *traffic sign*, *traffic lights*. We add a new *chargepads* class to the baseline. Segmentation task has *vehicles*, *pedestrians*, *cyclists*, *road*, *lanes*, and *curbs* categories. The depth task provides scale-aware distance in 3D space. The model is trained jointly using the public WoodScape [26] dataset comprising 8k samples and evaluated on 2k samples, augmented by our chargepad data.



Fig. 3: Various different commercial chargepads. Images are taken from [\[link1\]](#) [\[link2\]](#) [\[link3\]](#).



Fig. 4: ArUco patterns on a charging station

In computer vision and machine learning, any object of interest is first trained, and the model will later predict the similar object by classification and/or detection. It is known that data collection and training is a highly time-consuming process. Given the exploding growth of electric vehicles and still non-standardized chargepads, it is impossible to gather all chargepad types and train a robust model. Hence, we will have to deal with unknown chargepads via the online self-supervised learning described in this paper. For online learning, we must first learn about the surrounding environment and isolate our object of interest-based on the semantic segmentation, object detection, and depth estimation of the scene shown in Figure 14. That is, we use these cues to filter regions of the image that are non-chargepad related.

Briefly summarizing the loss functions used for training, we construct a self-supervised monocular structure-from-motion (SfM) system for distance and pose estimation. The total loss consists of a photometric term \mathcal{L}_r , a smoothness term \mathcal{L}_s , that enforces edge-aware smoothness within the distance map \hat{D}_t , a cross-sequence distance consistency loss \mathcal{L}_{dc} , and feature-metric losses from [27] where \mathcal{L}_{dis} and \mathcal{L}_{cvt} are computed on I_t . The final loss function for distance estimation is a weighted average of all these losses. The segmentation task contains seven classes on the WoodScape and employs *Lovasz-Softmax* [28] loss. Motion segmentation employs two frames and predicts either a binary moving or static mask and also employs *Lovasz-Softmax* and *Focal* [29] loss for managing class imbalance instead of the cross-entropy loss. For object detection, we make use of YOLOv3 loss [30] and add IoU loss using segmentation mask [13].

The chargepad is first detected by the object detection part of our three task network as described in Figure 5. Like any other vision-based approach, our chargepad detection also suffers from issues like varying lighting and weather conditions, shadows [31], and the wear and tear of the pattern itself. So consistent detection of chargepad in each frame is not guaranteed. So it is beneficial to track the previously detected bounding boxes so that we can predict the relative position of the chargepad in the instances of no detection in some frames.

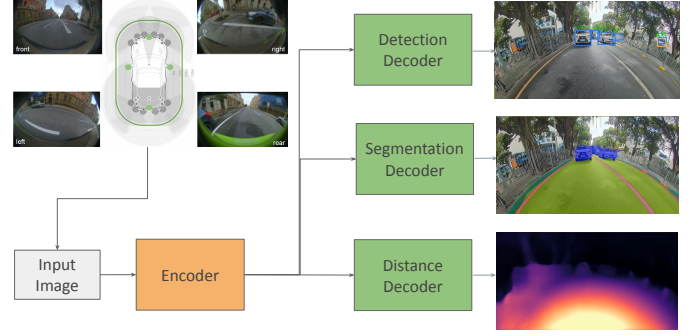


Fig. 5: Three task perception stack

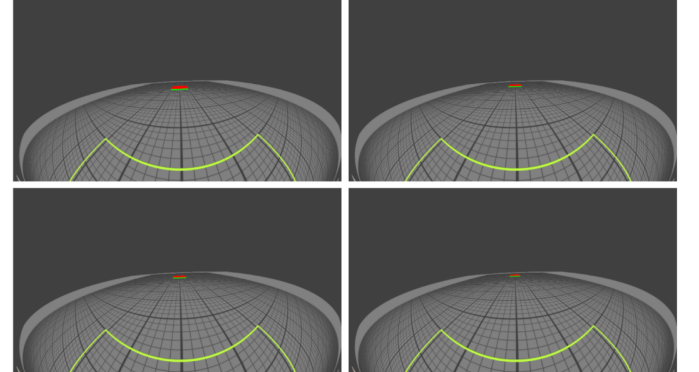


Fig. 6: Synthetic analysis of the pixel size of chargepads at various distances from the vehicle.

We use SORT [32] for online and real-time tracking of the detected chargepad. Once the bounding box is detected and tracked, the vehicle's angle towards the detected chargepad is estimated based on our previous work [33].

As the pattern looks relatively small when the vehicle is far, the detection will only start when the vehicle approaches a reasonable distance from the chargepad. To analyze this, we modeled what a typically sized chargepad (60cm \times 60cm) looks like in a fisheye image, as shown in Figure 6. The size in the image at various distances is given in Table I. The image height of the chargepad is only 12 pixels at 6m, which we expect to be the upper limit of detection (this is analyzed later in §III).

C. Online Self-supervised Learning

The fundamental problem with the conventional offline trained machine learning approach is the inability of the computer vision network (the deep learning model) to identify the non trained classes of objects at inference time. Specifically, for our proposed architecture, this means that it is impossible

Distance (m)	Size (pixels)
3	100 × 31
4	81 × 23
5	65 × 20
6	54 × 12

TABLE I: Study of resolution of chargepad at different locations simulating a 2Mpix fisheye camera and a target of 900x800x70 mm.

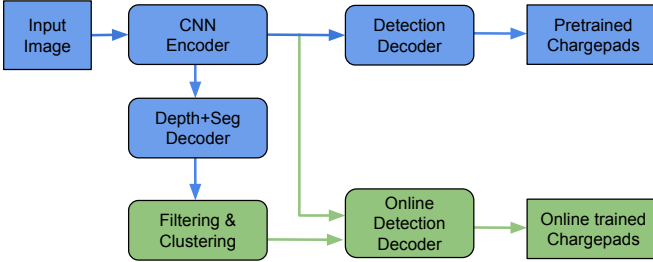


Fig. 7: Illustration of online learning framework. Blue blocks denote the offline trained model. Green blocks denote the online training model, which uses post-processing of depth and segmentation guiding by backtracking of the driver's final position of chargepad location.

to cover all types of chargepad objects before deployment. In situations where a previously unseen chargepad is visible in the scene, there is a strong probability that the network might make a random prediction and cause a failure. An extensive set of research work is carried out looking for possibilities for unsupervised learning in different domains. Paper [34] uses a two-stage method, first finding the nearest neighbors of each image with feature similarity and then using that information for a learnable approach for image classification. Similarly, [35] proposed to learn image features by training Convolution Nets to recognize the 2D rotation applied to the image to achieve Unsupervised Representation Learning. An important thing to note is that most successful deep learning networks are supervised learning algorithms so far. However, rapid growth in the interest of unsupervised learning could soon close the gap. Supervised learning is typically used as the basis for examining the performance of any self-supervised, or semi-supervised model [36]. It means they require fully or partially annotated data for optimal training of the network.

This makes the problem of online learning of unknown class entities even harder to achieve optimal performance; online data needs to be annotated before the learning process, resulting in a significant cost overhead if not done automatically. Without automation, it involves the data collection for various types of chargepads, annotation of data by trained annotators, and re-training of the deep learning algorithms to adapt to the online data. For previously unseen chargepads, this requires data to be transferred from the vehicle to a facility where manual annotation can occur, the network to be re-trained, and to be downloaded again to the vehicle. All of these steps are costly and difficult to implement. This makes the goal of online auto-annotation much more attractive.

Figure 7 illustrates our proposed online learning framework. During the deployment time, the offline detector detects the



Fig. 8: Examples of visual features in an image. The exact features depend on the feature Extraction and Description algorithm used [42].

pre-trained class of entities as usual. The online detector warns the end-user when they attempt to engage the auto-alignment, but it fails due to a failure to detect a previously unseen chargepad. The driver must then manually complete the alignment. However, as described later, this manual alignment is used to provide the auto-annotation for online learning.

D. Visual SLAM based Environment Localization

Simultaneous localization and mapping (SLAM) is a technique for estimating sensor motion and reconstructing structure in an unknown environment. When a camera is (or multiple cameras are) used for this purpose, it is called Visual SLAM. The vision sensor can be a monocular, stereo vision, Omnidirectional (360-degree), or Red Green Blue Depth (RGBD) camera. Visual SLAM is composed of mainly three modules: initialization, tracking, and mapping. Both [37] and [38] both provide an extensive surveys of Visual SLAM techniques. Feature-based techniques are where a set of features (e.g., edges [39] or corners [40]) are extracted from the input images and matched to the same features obtained from different poses and minimize the re-projection error. On the other hand, the direct Visual SLAM (e.g., [41]) technique compares the entire images to each other by minimizing photometric error.

We base our Visual SLAM enhancement for chargepad alignment on previous work on trained parking using SLAM [19]. In the next section, we describe the overall Visual SLAM architecture employed in the proposed system. However, it is pertinent to provide some details here, though the reader is referred to [19] for complete details. The motivation is illustrated in Figure 8 where feature locations (marked in red boxes) relative to the chargepad (marked in the blue box) are found. This will enable localization at a farther distance when the chargepad is poorly visible.

The trained trajectory following operates in two distinct phases: training and replay. During training, the driver manually drives to the chargepad location (within the range of the chargepad detector described above). Visual features are extracted from the video stream and matched between frames. ORB-based SLAM [43] has become almost standard in many applications. However, we have found that AKAZE [44] is a more robust feature for the replay phase, and as such, we use AKAZE for the feature extraction and matching. The

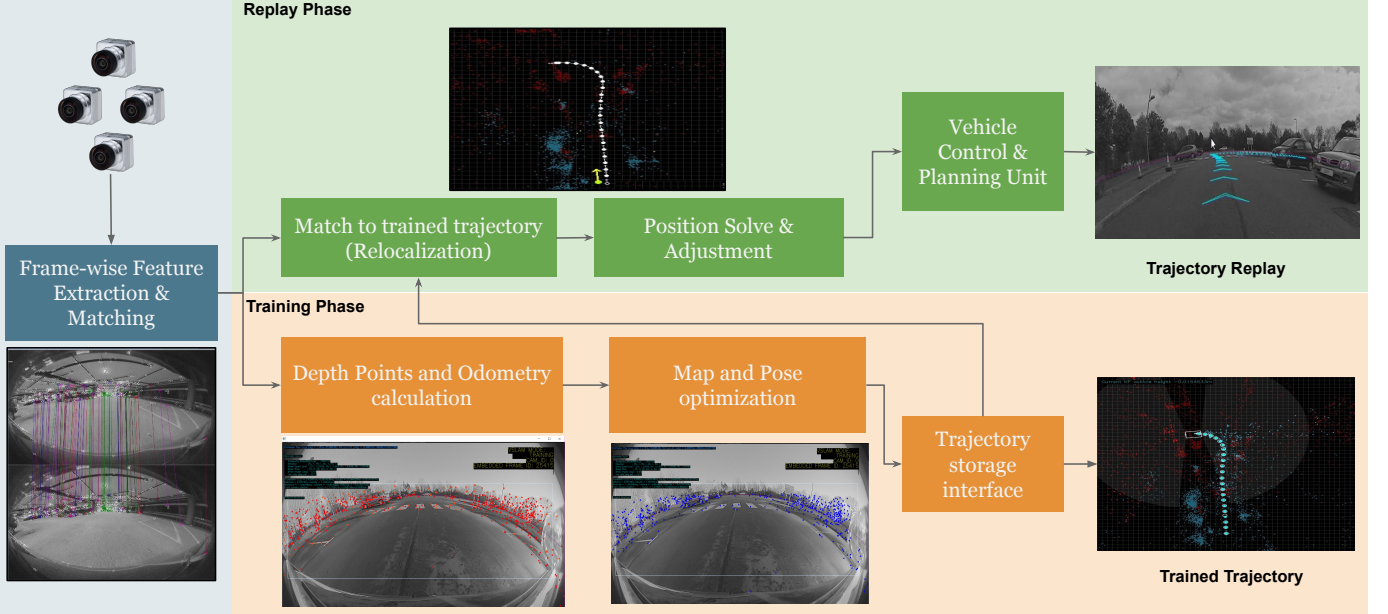


Fig. 9: Visual SLAM training and relocalization architecture [19].

end goal of the SLAM approach is bundle-adjustment, that is, using Levenberg-Marquardt to iteratively refine the 3D location of the features and the position of the vehicle across the entire trajectory (e.g., Figure 10). However, any iterative method benefits from having a decent seed. As such, we deploy a visual odometry and feature triangulation to give an initial estimate of the scene structure. As we are only looking for a seed for the bundle adjustment, we employ nothing more complex than the monocular 5-point algorithm for visual odometry [45] and the direct linear method of reconstruction [46]. For a complete review of visual odometry techniques, the reader is referred to [47]. For further discussion on optimal triangulation approaches, the reader is referred to [46]. The output of visual odometry and triangulation is bundle adjusted using a windowed approach [38]. Each window has an associated keyframe.

The appropriately trained trajectory is loaded in the replay phase, and the recorded bundle-adjusted keyframe feature descriptors are scanned and matched to visual features extracted from the current frame. Levenberg-Marquardt is then used here again. However, this time, only the vehicle's position is solved (as the 3D structure is resolved during the training phase). Figure 9 shows the overall architecture of the VSLAM pipeline.

It should be noted that the term "training" here may cause some confusion for readers. In this case, we mean training in a more general sense, and it does not equate with training in machine learning terminology. Currently, we rely solely on classical computer vision for our SLAM and do not use any machine learning in this part of our architecture proposal. However, we do note recent advances in that area [48].

E. Overall Architecture

In previous sections, we have discussed individual building blocks of the proposed approach. In this section, we will

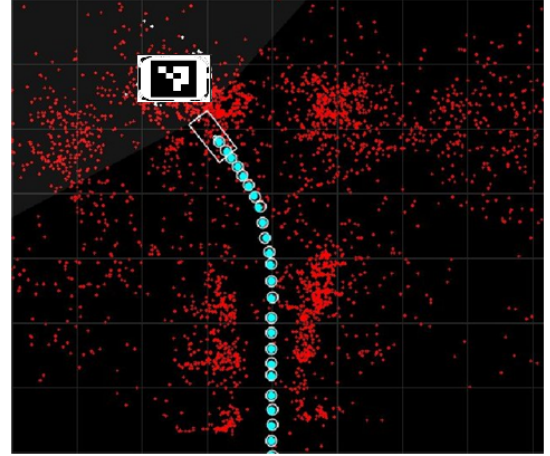


Fig. 10: 3D feature layout for a single trajectory.

discuss the overall architecture of our proposed system, which is shown in Figure 11. We will explain each of the stages. Firstly, a Global Positioning System (GPS) or Human-Machine Interface (HMI) *Trigger* prompts the system. For example, GPS can tell that the host vehicle is in the vicinity of the chargepad and thus triggers an attempt at detecting and aligning the vehicle with the chargepad. Alternatively, this trigger can be done via user input. If the pre-trained MTL detection network recognizes a chargepad (per Figure 7), then the host vehicle can proceed with the alignment. It should be noted that MTL Encoder is mentioned several times in Figure 11; however, it is just a single encoder that is running.

The mechanisms of vehicle alignment and control are not the subject of this paper; however, vehicle control is a reasonably well-understood problem for several decades [49], though there is more recent research in the topic [50]. In Figure 11, we show a high level description of that the *Vehicle-Chargepad Alignment* implementation would look like. Given an initial detection and localization of the chargepad, the trajectory

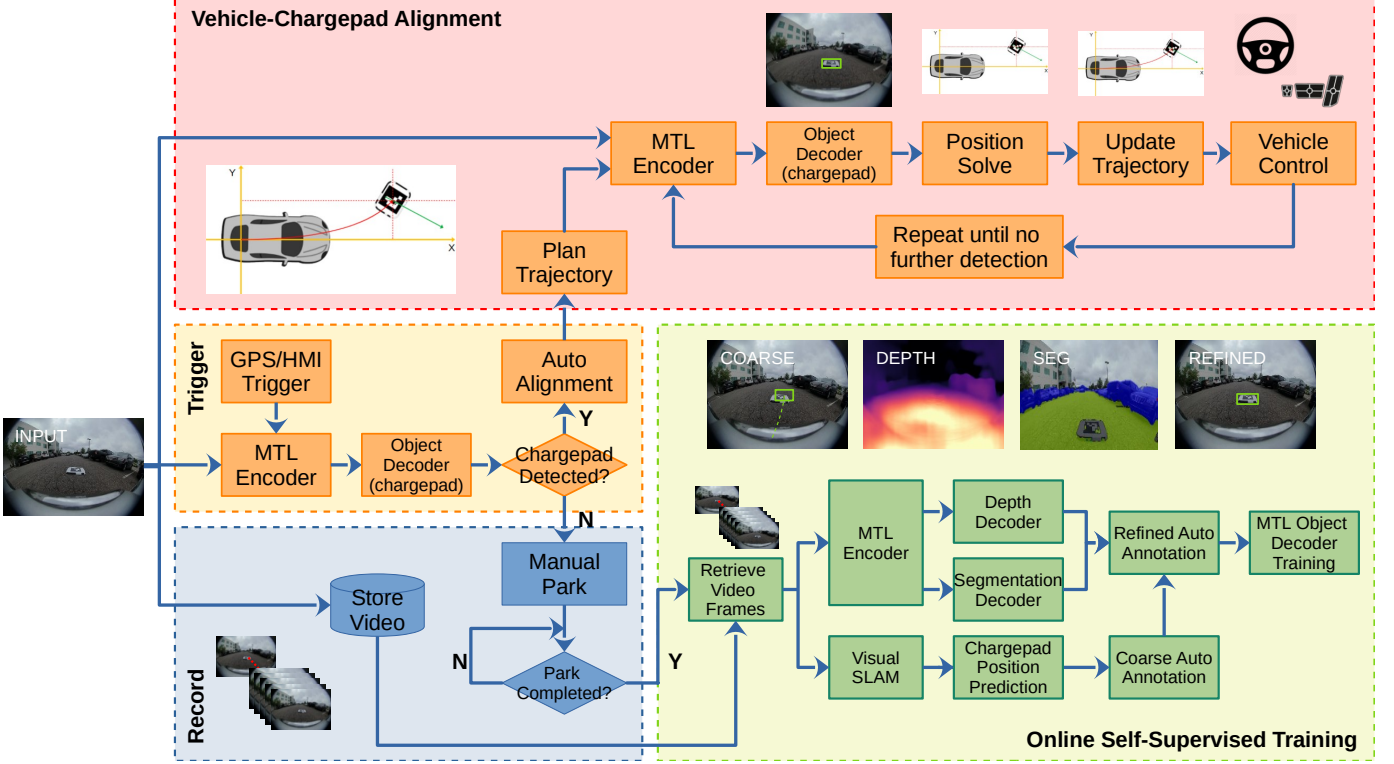


Fig. 11: Overall system architecture for online chargepad learning and vehicle-chargepad alignment.

that the vehicle should follow can be calculated. To account for drift, the trajectory can be iteratively updated based on further chargepad detections, which will account for any drift. Eventually, the chargepad will pass out of the view of the cameras (e.g. when it passes under the body of the vehicle). The vehicle will rely solely on odometry to guide it to the final position.

In the case that the pre-trained network fails to detect a chargepad (for example, if the chargepad we are attempting to detect is not of a type in the pre-trained network dataset), unfortunately, the user must manually align the vehicle with the pad. In this case, the system triggers the *record* of the video scenes alongside the manual alignment of the vehicle with the chargepad. Thus video frames from the point of engagement of the system through to park completion are available to the online training.

Once the vehicle has been manually parked, the recorded video frames are then available to the *online self-supervised training* algorithm. Video frames are retrieved from the storage in sequence, and Visual SLAM is used to predict the position of the chargepad in each frame of recorded video (Figure 12). However, due to issues with the accuracy of the manual alignment of the vehicle (as already discussed) and due to drift with odometry over time, this auto-annotation will have low accuracy. For that reason, we use road segmentation and depth outputs of the MTL network to refine the annotation ahead of training. Depth is used as a simple filter to remove any objects above the ground. The ground segmentation is used to refine the detection by filtering the ground surface, leaving just the chargepad as a refined detection. This refined auto-annotation of the chargepad objects can then be used to update the training

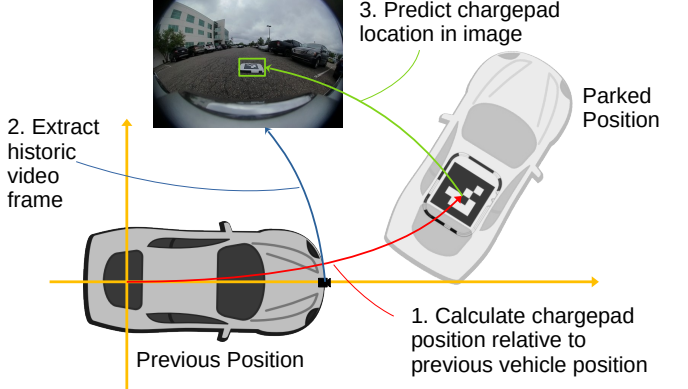


Fig. 12: Employing Visual SLAM/Odometry to predict the position of the chargepad in an image corresponding to a previous vehicle position.

of the MTL Object Decoder.

An issue with the approach outlined thus far is that the range of the chargepad detector is limited to a max of 5 to 6m (depending on configuration). This can impact the ability of the vehicle to align itself with the chargepad without overly complex maneuvers. The range can be extended by increasing the cameras' resolution, but this has other impacts at a system level, not least the cost of the system. A Visual SLAM-based relocalization pipeline can be used in this case, as discussed earlier. Figure 9, shows a high level architecture for a relocalisation algorithm. A trajectory is learned by the extraction of visual features and map and pose optimization. The trajectory, including visual feature descriptors, is stored. In the replay phase, features extracted from the live video



Fig. 13: End user driver view on HMI.

stream are matched to the stored features. This matching is then used to solve for the position of the vehicle against the stored trajectory. The role of path planning and vehicle control is to guide the vehicle to join and follow the previously-stored trajectory. The general approach of relocalization against a pre-trained trajectory is described in more detail in [19].

In this case, we can deploy the VSLAM-based relocalization to extend the range of the chargepad alignment. When the chargepad alignment functionality is triggered, we first search for the chargepad itself using the MTL output. In the case that this fails, the system will then attempt to match the pre-trained trajectory. The vehicle can then follow the pre-trained trajectory until the chargepad comes within range for direct detection and final alignment.

Finally, auto-alignment is not desired even in such a case (for example, in a vehicle that is not equipped with automated driving). As we propose, it is still desirable to generate HMI guidelines for the driver. We give an example of this in Figure 13. The HMI is used to guide the driver towards the chargepad and increase the accuracy of the manual alignment. Once the chargepad passes under the vehicle, we can still track the position of the chargepad using the known odometry of the vehicle.

III. RESULTS

A. Dataset

The chargepad training dataset comprises 375 sequences with roughly equal indoor and outdoor scenes. The test sequences were independently created from similar environments. Synthetic images were created with the chargepad to enable evaluation of additional road or pavement textures. The test set consists of 200 sequences with a split of 65 indoor, 64 outdoor, and 71 synthetic scenes. The dimensions of the chargepad used are 760mm×620mm×60mm. The images were both captured from front and rear cameras. This is because chargepad detection and tracking can be in both forward and reverse directions. The evaluation of synthetic images was purely based on only real image-based training to understand generalization to new road textures.

B. Evaluation

Firstly, Figure 14 shows the multi-task baseline results illustrating the performance of segmentation and depth estimation of the chargepad and its surroundings. Figure 15 illustrates the results of chargepad detection using the proposed method for

outdoor, indoor, and synthetic scenes. The blue bounding box represents the detected chargepad on the image. The detected class label "cpad" is also displayed along with the confidence of the prediction. We use a confidence threshold of 25% below which the detection is unreliable with false positives on other objects such as vehicles. We observe that 95% of the detections have greater than 50% confidence in the prediction. Figure 15 also illustrates reliable detection of chargepads at different ranges. To understand performance on various ground surface types, we also tested with a set of synthetic images (see the last row of Figure 15). The algorithm generalizes well from real to synthetic images.

Table II provides quantitative results of the detection performance using the average precision score on the test dataset with 0.8 IoU threshold. As it is a fixed ArUco pattern chargepad, the detection accuracy is high as expected. As expected, the proposed online training algorithm achieves roughly 8% lesser accuracy due to noisy supervision. We release the dataset to perform more research to close this gap. We also tested a simple OpenCV based ArUco detector, but it achieves poor performance, particularly for ranges beyond 3 meters.

For the previous experiments, we used the raw fisheye images without any undistortion. We explored normalization using top-view correction, mainly to improve the detection range. In Figure 16, we show a comparison of detecting the chargepad on raw fisheye and top-view. Top-view image improves the detection range significantly, as shown in Table III. However, it inhibits the usage of a shared encoder of the multi-task visual perception model. Thus, we also explore a top-view spatial transformer inspired by OFTNet [51]. We insert a spatial transformer block in between the encoder and YOLOv3 decoder. It slightly improves the detection range compared to the top-view corrected image. Finally, we show that the combination of Visual SLAM and CNN-based chargepad detection significantly increase the range compared to all other methods without requiring a top-view image transformation.

Getting the exact alignment of the vehicle with the chargepad is difficult, as no automated ground truth data was readily available. However, we manually evaluated the final alignment of the vehicle against the chargepad on a small number of scenes (three indoor and three outdoor scenes), as presented in Table IV. It can be seen that at least five of the six scenes tested, we are within the $\pm 10\text{cm}$ alignment accuracy required for optimal charging [4], with the final scene being only just outside. It would seem that the alignment accuracy is slightly higher for indoor scenes, as the lighting tends to be more controlled. Additionally, in indoor scenes, the ground surface tends to be more even, reducing odometry drift when

Method	Average Precision (IoU 0.80)		
	Indoor	Outdoor	Synthetic
Baseline offline learning	93.5	98.9	95.3
OpenCV ArUco detector	58.8	65.7	62.3
Proposed online learning	85.5	90.3	87.9

TABLE II: Comparative study of different approaches.



Fig. 14: Detection of chargepad using depth and segmentation.

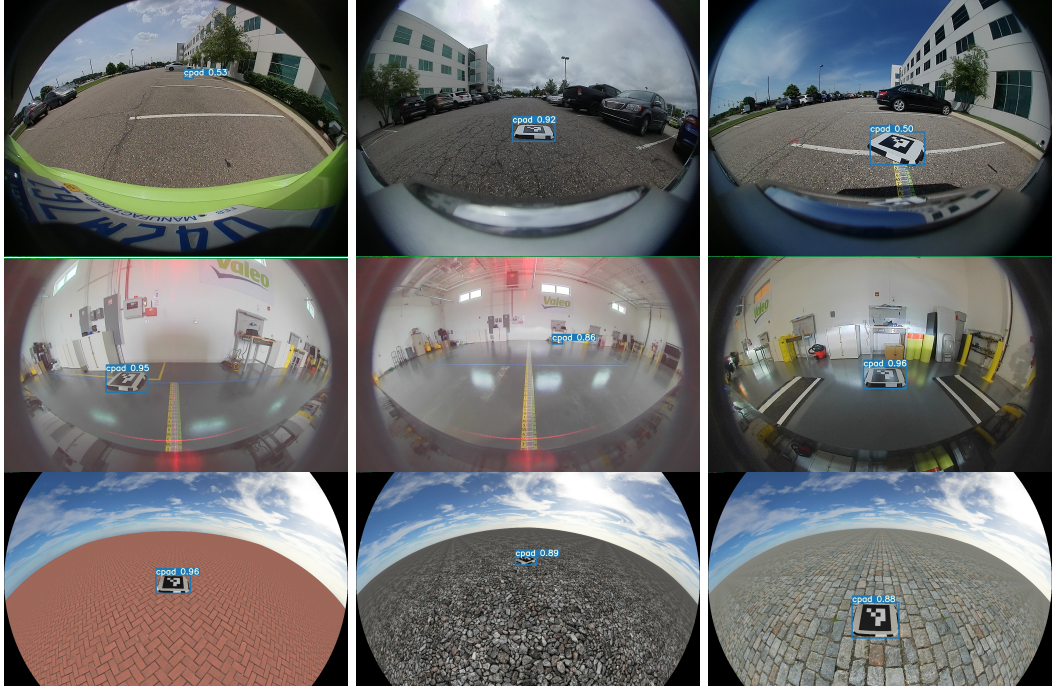


Fig. 15: Qualitative results of chargepad Detection and Tracking in different scenarios namely outdoor (top), indoor (middle) and synthetic (bottom).



Fig. 16: Top: Detection on regular fish-eye image view. Bottom: Detection on top view corrected image.

the chargepad is under the vehicle and no longer detected.

Input	Average Range (m)
Fisheye	5.2
Top-view corrected	6.8
Top-view spatial transformer	7.1
Fisheye + VSLAM	12.3

TABLE III: Range study of different input representations.

IV. CONCLUSION

In this paper, we explored the application of wireless charging assistance for electric vehicles using widely available surround-view camera systems. Accurate alignment of the vehicle with the inductive chargepad is known to be critical for efficient charging. However, while visual techniques for alignment make much sense, not least due to the proliferation of cameras on vehicles in general, unseen chargepad designs will cause failure. We have proposed an online learning architecture to be scalable to any type of chargepad, using

Type	Scene	Positional Offset (cm)	Angular Offset (deg)
Indoor	Scene 1	4.7	4.3
	Scene 2	3.6	5.5
	Scene 3	3.0	5.1
Outdoor	Scene 4	10.8	8.7
	Scene 5	9.0	9.2
	Scene 6	8.9	10.1

TABLE IV: Localization and alignment accuracy in terms of final positional and angular offset.

the known vehicle trajectory, augmented by object detection, semantic segmentation, and depth estimation, to auto-annotate unseen chargepads. Thus, when confronted with a previously unseen chargepad, the driver should only have to park once manually. Due to range limitations with the detection, we have also proposed an enhancement to using a visual SLAM localization method. Using this combination of approaches, we have demonstrated an effective solution. We will release a portion of the dataset to encourage further research in this area.

ACKNOWLEDGMENT

The authors would like to thank Mirian Rodriguez-Romero for providing some of the ArUco based chargepad videos used for training and validation in this paper. Thanks to Nivedita Tripathi for input on the Visual SLAM topics.

REFERENCES

- [1] N. Rietmann, B. Hügler, and T. Lieven, “Forecasting the trajectory of electric vehicle sales and the consequences for worldwide CO₂ emissions,” *Journal of Cleaner Production*, vol. 261, p. 121038, 2020.
- [2] SAE International, “J2954: Wireless power transfer for light-duty plug-in/electric vehicles and alignment methodology,” 2020.
- [3] F. He, Y. Yin, and J. Zhou, “Integrated pricing of roads and electricity enabled by wireless power transfer,” *Transportation Research Part C: Emerging Technologies*, vol. 34, pp. 1–15, 2013.
- [4] S. A. Birrell, D. Wilson, C. P. Yang, G. Dhadyalla, and P. Jennings, “How driver behaviour and parking alignment affects inductive charging systems for electric vehicles,” *Transportation Research Part C: Emerging Technologies*, vol. 58, pp. 721–731, 2015.
- [5] W. Ni, I. B. Collings, X. Wang, R. P. Liu, A. Kajan, M. Hedley, and M. Abolhasan, “Radio alignment for inductive charging of electric vehicles,” *IEEE Transactions on Industrial Informatics*, vol. 11, no. 2, pp. 427–440, 2015.
- [6] A. Babu and B. George, “Sensor system to aid the vehicle alignment for inductive EV chargers,” *IEEE Transactions on Industrial Electronics*, vol. 66, no. 9, pp. 7338–7346, 2019.
- [7] J. Tiemann, J. Pillmann, S. Bocker, and C. Wietfeld, “Ultra-wideband aided precision parking for wireless power transfer to electric vehicles in real life scenarios,” in *2016 IEEE 84th Vehicular Technology Conference (VTC-Fall)*, 2016, pp. 1–5.
- [8] R. Senju, H. Omori, D. Uchimoto, T. Morizane, and N. Kimura, “A new position detecting method for wireless EV chargers,” in *2019 8th International Conference on Renewable Energy Research and Applications (ICRERA)*, 2019, pp. 810–814.
- [9] M. Heimberger, J. Horgan, C. Hughes, J. McDonald, and S. Yogamani, “Computer vision in automated parking systems: Design, implementation and challenges,” *Image and Vision Computing*, vol. 68, pp. 88–101, 2017.
- [10] L. Liu, P. Niu, D. Luo, Y. Guo, and Y. Sun, “A method for aligning of transmitting and receiving coils of electric vehicle wireless charging based on binocular vision,” in *2017 IEEE Conference on Energy Internet and Energy System Integration (EI2)*, 2017, pp. 1–6.
- [11] Y.-C. Liu, K.-Y. Lin, and Y.-S. Chen, “Bird’s-eye view vision system for vehicle surrounding monitoring,” in *Proceedings of the International Workshop on Robot Vision (RobVis)*, G. Sommer and R. Klette, Eds., 2008.
- [12] C. Eising, J. Horgan, and S. Yogamani, “Near-field sensing architecture for low-speed vehicle automation using a surround-view fisheye camera system,” *IEEE Transactions on Intelligent Transport Systems*, 2021, under review; preprint available at <https://arxiv.org/abs/2103.17001>.
- [13] H. Rashed, E. Mohamed, G. Sistu, V. Ravi Kumar, C. Eising, A. El-Sallab, and S. Yogamani, “Generalized Object Detection on Fisheye Cameras for Autonomous Driving: Dataset, Representations and Baseline,” in *Proceedings of the IEEE/CVF Winter Conference on Applications of Computer Vision*, 2021, pp. 2272–2280.
- [14] M. Uricar, G. Sistu, H. Rashed, A. Vobecsky, V. R. Kumar, P. Krizek, F. Burger, and S. Yogamani, “Let’s get dirty: Gan based data augmentation for camera lens soiling detection in autonomous driving,” in *Proceedings of the IEEE/CVF Winter Conference on Applications of Computer Vision*, 2021, pp. 766–775.
- [15] V. R. Kumar, S. Milz, C. Witt, M. Simon, K. Amende, J. Petzold, S. Yogamani, and T. Pech, “Monocular fisheye camera depth estimation using sparse lidar supervision,” in *2018 21st International Conference on Intelligent Transportation Systems (ITSC)*. IEEE, 2018, pp. 2853–2858.
- [16] V. Ravi Kumar, S. A. Hiremath, M. Bach, S. Milz, C. Witt, C. Pinard, S. Yogamani, and P. Mäder, “Fisheyedistancenet: Self-supervised scale-aware distance estimation using monocular fisheye camera for autonomous driving,” in *2020 IEEE International Conference on Robotics and Automation (ICRA)*. IEEE, 2020, pp. 574–581.
- [17] V. Ravi Kumar, S. Yogamani, M. Bach, C. Witt, S. Milz, and P. Mäder, “UnRectDepthNet: Self-Supervised Monocular Depth Estimation using a Generic Framework for Handling Common Camera Distortion Models,” in *IEEE/RSJ International Conference on Intelligent Robots and Systems, IROS 2020, Las Vegas, NV, USA, October 24, 2020 - January 24, 2021*. IEEE, 2020, pp. 8177–8183.
- [18] V. Ravi Kumar, M. Klingner, S. Yogamani, S. Milz, T. Fingscheidt, and P. Mäder, “Syndistnet: Self-supervised monocular fisheye camera distance estimation synergized with semantic segmentation for autonomous driving,” in *Proceedings of the IEEE/CVF Winter Conference on Applications of Computer Vision*, 2021, pp. 61–71.
- [19] N. Tripathi and S. Yogamani, “Trained trajectory based automated parking system using Visual SLAM,” in *Proceedings of the IEEE/CVF Conference on Computer Vision and Pattern Recognition (CVPR) Workshops*, 2021.
- [20] G. Sistu, I. Leang, S. Chennupati, S. Yogamani, C. Hughes, S. Milz, and S. Rawashdeh, “Neural: Towards a unified visual perception model for automated driving,” in *2019 IEEE Intelligent Transportation Systems Conference (ITSC)*. IEEE, 2019, pp. 796–803.
- [21] M. Kalaitzakis, B. Cain, S. Carroll, A. Ambrosi, C. Whitehead, and N. Vitzilaios, “Fiducial markers for pose estimation,” *Journal of Intelligent & Robotic Systems*, vol. 101, no. 71, 2021.
- [22] S. Garrido-Jurado, R. Muñoz-Salinas, F. J. Madrid-Cuevas, and M. J. Marín-Jiménez, “Automatic generation and detection of highly reliable fiducial markers under occlusion,” *Pattern Recognition*, vol. 47, no. 6, pp. 2280–2292, 2014.
- [23] F. Romero-Ramirez, R. Muñoz-Salinas, and R. Medina-Carnicer, “Speeded up detection of squared fiducial markers,” *Image and Vision Computing*, vol. 76, 2018.
- [24] V. Ravi Kumar, S. Yogamani, H. Rashed, G. Sitsu, C. Witt, I. Leang, S. Milz, and P. Mäder, “Omnidet: Surround view cameras based multi-task visual perception network for autonomous driving,” *IEEE Robotics and Automation Letters*, vol. 6, no. 2, pp. 2830–2837, 2021.
- [25] K. He, X. Zhang, S. Ren, and J. Sun, “Deep residual learning for image recognition,” in *Proceedings of the IEEE/CVF Conference on Computer Vision and Pattern Recognition (CVPR)*, 2016, pp. 770–778.
- [26] S. Yogamani, C. Hughes, J. Horgan, G. Sistu, P. Varley, D. O’Dea, M. Uricar, S. Milz, M. Simon, K. Amende, *et al.*, “Woodscape: A multi-task, multi-camera fisheye dataset for autonomous driving,” in *Proceedings of the IEEE/CVF International Conference on Computer Vision*, 2019, pp. 9308–9318.
- [27] C. Shu, K. Yu, Z. Duan, and K. Yang, “Feature-metric loss for self-supervised learning of depth and egomotion,” in *European Conference on Computer Vision*. Springer, 2020, pp. 572–588.
- [28] M. Berman, A. R. Triki, and M. B. Blaschko, “The lovász-softmax loss: A tractable surrogate for the optimization of the intersection-over-union measure in neural networks,” in *Proceedings of the IEEE Conference on Computer Vision and Pattern Recognition*, 2018, pp. 4413–4421.
- [29] T.-Y. Lin, P. Goyal, R. Girshick, K. He, and P. Dollár, “Focal loss for dense object detection,” in *Proceedings of the IEEE/CVF International Conference on Computer Vision*, 2017, pp. 2980–2988.
- [30] J. Redmon and A. Farhadi, “YOLOv3: An incremental improvement,” *arXiv preprint arXiv:1804.02767*, 2018.

- [31] L. Yahiaoui, J. Horgan, B. Deegan, S. Yogamani, C. Hughes, and P. Denny, "Overview and empirical analysis of isp parameter tuning for visual perception in autonomous driving," *Journal of Imaging*, vol. 5, no. 10, 2019.
- [32] L.-G. C. Keng-Chi Liu, Yi-Ting Shen, "Simple online and realtime tracking with spherical panoramic camera," *2018 IEEE International Conference on Consumer Electronics (ICCE)*, pp. 1–6, 2018.
- [33] A. Dahal, J. Hossen, S. Chennupati, G. Sistu, K. Malhan, M. Amasha, and S. Yogamani, "Deeptrailerassist: Deep learning based trailer detection, tracking and articulation angle estimation on automotive rear-view camera," *IEEE/CVF International Conference on Computer Vision Workshop (ICCVW)*, 2019.
- [34] W. V. Gansbeke, S. Vandenbende, S. Georgoulis, M. Proesmans, and L. V. Gool, "Learning to classify images without labels," *CoRR*, vol. abs/2005.12320, 2020. [Online]. Available: <https://arxiv.org/abs/2005.12320>
- [35] S. Gidaris, P. Singh, and N. Komodakis, "Unsupervised representation learning by predicting image rotations," in *6th International Conference on Learning Representations, ICLR 2018*, 2018.
- [36] L. Beyer, X. Zhai, A. Oliver, and A. Kolesnikov, "S⁴L: Self-supervised semi-supervised learning," in *Proceedings of the IEEE/CVF International Conference on Computer Vision (ICCV)*, 2019, pp. 1476–1485.
- [37] T. Taketomi, H. Uchiyama, and S. Ikeda, "Visual SLAM algorithms: a survey from 2010 to 2016," *IPSJ Transactions on Computer Vision and Applications*, vol. 9, no. 16, 2017.
- [38] F. Fraundorfer and D. Scaramuzza, "Visual odometry : Part ii: Matching, robustness, optimization, and applications," *IEEE Robotics and Automation Magazine*, vol. 19, no. 2, pp. 78–90, 2012.
- [39] F. Schenk and F. Fraundorfer, "RESLAM: A real-time robust edge-based slam system," in *Proceedings of the International Conference on Robotics and Automation (ICRA)*, 2019, pp. 154–160.
- [40] W. Y. Jeong and K. M. Lee, "Visual slam with line and corner features," in *Proceedings of the IEEE/RSJ International Conference on Intelligent Robots and Systems (IROS)*, 2006, pp. 2570–2575.
- [41] D. Caruso, J. Engel, and D. Cremers, "Large-scale direct SLAM for omnidirectional cameras," in *Proceedings of the IEEE/RSJ International Conference on Intelligent Robots and Systems (IROS)*, 2015.
- [42] E. Salahat and M. Qasaimeh, "Recent advances in features extraction and description algorithms: A comprehensive survey," in *2017 IEEE international conference on industrial technology (ICIT)*. IEEE, 2017, pp. 1059–1063.
- [43] R. Mur-Artal, J. M. M. Montiel, and J. D. Tardós, "Orb-slam: A versatile and accurate monocular slam system," *IEEE Transactions on Robotics*, vol. 31, no. 5, pp. 1147–1163, 2015.
- [44] P. F. Alcantarilla and T. Solutions, "Fast explicit diffusion for accelerated features in nonlinear scale spaces," *IEEE Transactions on Pattern Analysis and Machine Intelligence*, vol. 34, no. 7, pp. 1281–1298, 2011.
- [45] D. Nister, "An efficient solution to the five-point relative pose problem," in *Proceedings of the IEEE/CVF Computer Society Conference on Computer Vision and Pattern Recognition (CVPR)*, vol. 2, 2003, pp. II–195.
- [46] R. Hartley and A. Zisserman, *Multiple view geometry in computer vision*. Cambridge, 2003.
- [47] K. Yousif, Bab-Hadiashar, A., and R. Hoseinnezhad, "An overview to visual odometry and visual slam: Applications to mobile robotics," *Intelligent Industrial Systems*, vol. 1, pp. 289–311, 2015.
- [48] G. Li, L. Yu, and S. Fei, "A deep-learning real-time visual slam system based on multi-task feature extraction network and self-supervised feature points," *Measurement*, vol. 168, p. 108403, 2021.
- [49] R. E. Fenton, "Automatic vehicle guidance and control—a state of the art survey," *IEEE Transactions on Vehicular Technology*, vol. 19, no. 1, pp. 153–161, 1970.
- [50] E. Alcalá, V. Puig, J. Quevedo, T. Escobet, and R. Comasolivas, "Autonomous vehicle control using a kinematic Lyapunov-based technique with LQR-LMI tuning," *Control Engineering Practice*, vol. 73, pp. 1–12, 2018.
- [51] T. Roddick, A. Kendall, and R. Cipolla, "Orthographic feature transform for monocular 3d object detection," *British Machine Vision Conference*, 2019.



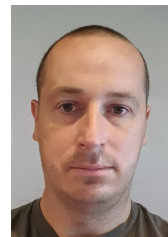
Ashok Dahal, Ph.D. has been working as a Senior Computer Vision Software Engineer at Valeo North America Inc. (Valeo) since 2015. Dr. Dahal's work at Valeo involves researching and developing ADAS features sold to major automobile companies worldwide. He is also involved in patent filing and Intellectual Property (IP) clearance process related to ADAS features and represents Valeo in various conferences and publications. Before joining Valeo, he completed his Ph.D. from University of North Texas, Denton, TX, with research focused on image and video analysis using computer vision and machine learning to improve colonoscopy video capabilities.



Varun Ravi Kumar received a B.E. degree in 2015 and an M.Sc. degree in 2017 from TU Chemnitz, Germany. He is currently a Ph.D. student in Deep Learning for autonomous driving affiliated to TU Ilmenau and is currently working at Valeo. His research is mainly focused on the design of self-supervised perception algorithms using neural networks for self-driving cars. His expertise lies in depth and flow estimation for fisheye images and multi-task modeling. His focus also lies in semantic, motion segmentation, 2D and 3D object detection, and point cloud processing. He was awarded the *Deutschlandstipendium* for top-class international talent. He was also part of Udacity's first cohort of Self-Driving-Car Nanodegree in 2017.



Senthil Yogamani is an Artificial Intelligence architect and holds a director-level technical leader position at Valeo Ireland. He leads the research and design of AI algorithms for various modules of autonomous driving systems. He has over 14 years of computer vision and machine learning experience, including 12 years of industrial and automotive systems. He is an author of 100+ publications with 1700+ citations and 100+ inventions with 70 filed patent families. He serves on the editorial board of various leading IEEE automotive conferences, including ITSC and IV, and the advisory board of various industry consortia including Khronos, Cognitive Vehicles, and IS Auto. He is a recipient of the best associate editor award at ITSC 2015 and best paper award at ITST 2012.



Ciarán Eising obtained his Ph.D. in Electronic and Computer Engineering at the National University of Ireland in 2010. From 2009 to 2020, Ciarán has worked as a computer vision team lead and architect in Valeo Vision Systems, where he also held the title of Senior Expert. In 2016, he was awarded the position of Adjunct Lecturer in the National University of Ireland, Galway. In 2020, Ciarán joined the University of Limerick as a lecturer in Computer Engineering.